

EVALUATION OF NEUTRON PRODUCTION CROSS SECTIONS AND EMISSION SPECTRA IN THE PROTON-INDUCED REACTION OF C-12, FE-56, AND PB-208 UP TO 250 MEV

Young-Ouk LEE, Young-Sik CHO and Jonghwa CHANG

Nuclear Data Evaluation Lab., KAERI
P.O Box 105 Yusung, Taejon, Korea
yolee@lui.kaeri.re.kr ; jhchang@kaeri.re.kr

ABSTRACT

In the particle transport analysis of the target system of ADS, proton-induced nuclear data, especially neutron yields and neutron emission spectra, play a key role. In this paper, as part of KAERI high energy library task, we present evaluation of (p, xn) double-differential neutron emission spectra for C-12, Fe-56, and Pb-208 for energies up to 250 MeV which are important nuclear data in the ADS target.

1. INTRODUCTION

In the accelerator-driven system (ADS), a high-power particle accelerator produces energetic protons that interact with a heavy metal target to produce neutrons. The source neutrons are generated by direct impinging of the accelerator proton beam onto a target material in a process called spallation. In the particle transport analysis of the target system of ADS, proton-induced nuclear data, especially neutron yields and neutron emission spectra, play a key role [1].

There are two approaches to provide a link between the nuclear reaction physics and transport analysis in the spallation target. One is to perform the calculation of both microscopic nuclear reactions using intra-nuclear cascade (INC) model and macroscopic transport process by one integrated computer code such as LAHET and HERMES. The other is to provide ENDF6 format data library using nuclear model calculation and benchmark with available experimental data. The data libraries, after processed, can serve as input for deterministic or Monte Carlo particle transport codes [2].

Currently some evaluation works are underway for high energy proton-induced nuclear data. Among them, LA150 [3] and JENDL High Energy File have ENDF6 format, and are being actively updated and benchmarked. The LA150 library, regarded as the most comprehensive and adequate for the ADS transport simulation, has nuclear data for about 30

Table 1: Reference measurements of neutron double-differential emission spectra for incident proton energy above 100 MeV

Reaction	Principal Author	E_p [MeV]	Emission Angles [deg]
$^{12}\text{C}(p, xn)$	Meier [6]	113.0	7.5, 30, 60, 150
	Meier [7]	256.0	7.5, 30, 60, 150
$^{nat}\text{Fe}(p, xn)$	Meier [6]	113.0	7.5, 30, 60, 150
	Meier [7]	256.0	7.5, 30, 60, 150
$^{208}\text{Pb}(p, xn)$	Scobel [8]	120.0	0 - 145 (14 angles)
	Scobel [8]	160.3	0 - 145 (14 angles)
	Scobel [9]	256.0	7.5, 30, 60, 150
	Stamer [10]	256.0	7.5, 30, 60, 150

important isotopes extending the neutron and proton energies up to 150 MeV. Meanwhile, the Korea Atomic Energy Research Institute (KAERI) is building high energy neutron-, proton-, and photon-induced nuclear data libraries for energies up to several hundreds of MeV (250 MeV [1] and 400 MeV [4]) in response to nuclear data needs from various R&Ds and applications.

In this paper, as part of KAERI high energy library task, we present our evaluation of proton-induced neutron production cross sections and emission spectra for C-12, Fe-56, and Pb-208 up to 250 MeV of incident protons, which are important nuclear data in the ADS target.

2. EVALUATION METHODS AND MODELS

2.1 REFERENCE MEASUREMENTS

Most of measurements for energies below 150 MeV referenced in the LA150 evaluation were also adopted in the present evaluation, and details are found in [5, 4]. Additionally, important measurements of neutron emission spectra for above 100 MeV of incident proton energy are referenced such as Meier [6, 7], Scobel [8, 9], and Stamer [10]. These five sets of measurements, listed in Table 2, provided important guidances in evaluating energy-angle spectra of emitted neutron for energies above 150 MeV. Electronic version of the measured data were retrieved from EXFOR database [11].

2.2 THEORETICAL MODELS

The optical model supplies particle transmission coefficients for Hauser-Feshbach statistical theory analysis used in nuclear data evaluations. In this work, the energy dependent potential depths for neutron and proton were adopted from the previous work of KAERI high energy library evaluation task [5] for neutrons and protons energies up to 400 MeV. Deuterons, tritons and alpha particle potentials employed in the LA150 were also adopted

for the emission of composite particles. Direct reaction contributions to inelastic scattering from low-lying discrete states were provided by a DWBA calculation with deformation parameters or a coupled-channel calculation with appropriate collective models.

For the emission reaction the latest version of the GNASH code [12] has been used to calculate nuclear reaction cross sections using the Hauser-Feshbach theory for equilibrium decay and the exciton model for preequilibrium decay. The exciton model was used to describe the processes of preequilibrium emission, and damping to equilibrium, during the evolution of the reaction. The file of discrete level information and ground-state masses, spin and parities was provided [13]. The mass values were based upon 1995 Audi compilation [14], and supplemented in the case of unmeasured masses with values from the Moeller and Nix calculations [15]. The Ignatyuk [16] nuclear level densities are used, which include the washing-out of shell effects with increasing excitation energy, and are matched continuously onto low-lying experimental discrete levels.

3. RESULTS AND COMPARISONS

In order to give overview of our evaluation results, Figure 1 provides 3-dimensional plots of the emission spectra information of neutrons. These plots, for protons incident on ^{12}C , ^{56}Fe , and ^{208}Pb , are combining of nonelastic cross sections, multiplicities (yields), and angle-integrated energy distributions evaluated in the present work. It shows the trends of increasing high-energy preequilibrium emission with increasing incident proton energy.

3.1 ^{12}C

In addition to its importance in medical applications, ^{12}C is an important element in accelerator-driven systems as a beam-stop material. For 113 MeV of incident proton, Fig. 2 compares our evaluation of double-differential neutron emission spectra at 7.5, 30, 60, and 150 degrees with the measurements of Meier et al. [6], together with the LA150 evaluation. In Fig. 3, evaluated energy-angle spectra of emitted neutrons for 256 MeV of incident proton are compared with the Meier et al.'s data measured in 1992 [7], giving overall agreements.

3.2 ^{56}Fe

The importance of ^{56}Fe in the ADS nuclear data is in its abundance in the target and the blanket designs. For 113 MeV of incident proton, Fig. 4 shows excellent agreements among our evaluation, LA150, and the measurements [6] for double-differential neutron emission spectra at 7.5, 30, 60, and 150 degrees. In Fig. 5, evaluated energy-angle spectra of emitted neutrons for 256 MeV of incident proton are compared with the measurements [7], providing quite good agreements for the entire energies and angles of emitting neutrons.

3.3 ^{208}Pb

The development of high-quality nuclear data for ^{208}Pb is particularly important due to lead's role as a spallation target and neutron multiplier in many ADS designs. Figure 6

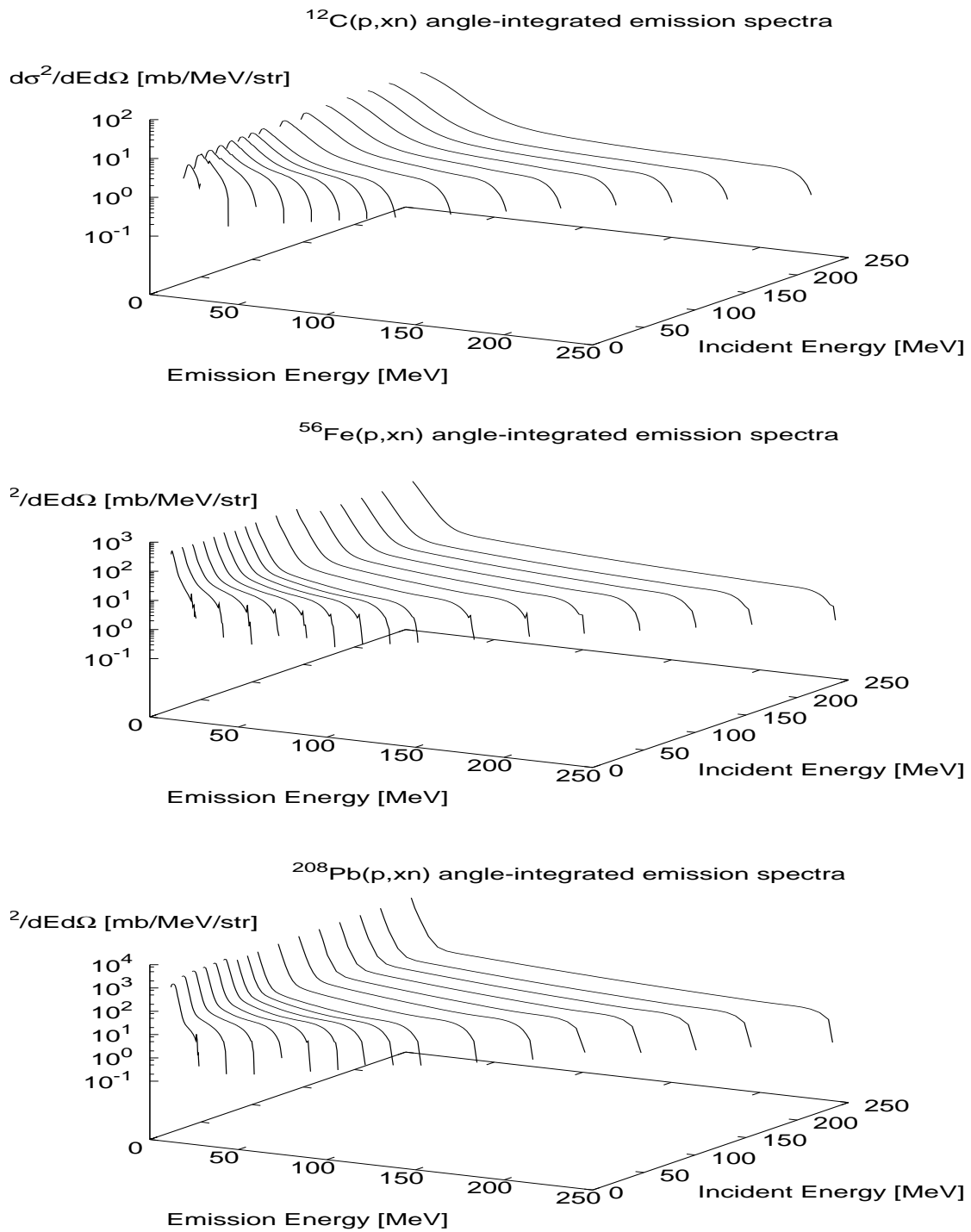


Figure 1: Evaluated angle-integrated neutron emission spectra for ^{12}C , ^{56}Fe , and ^{208}Pb reactions

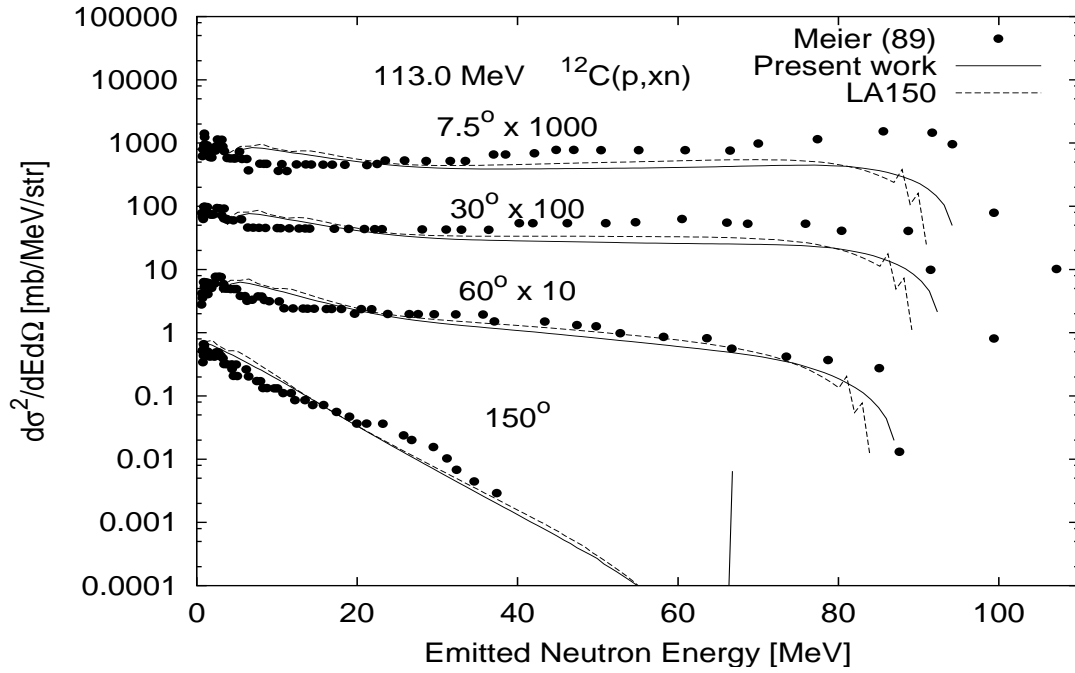


Figure 2: Evaluated $^{12}\text{C}(p, xn)$ double-differential neutron emission spectra compared with experimental data [6] and LA150 at 113 incident energy

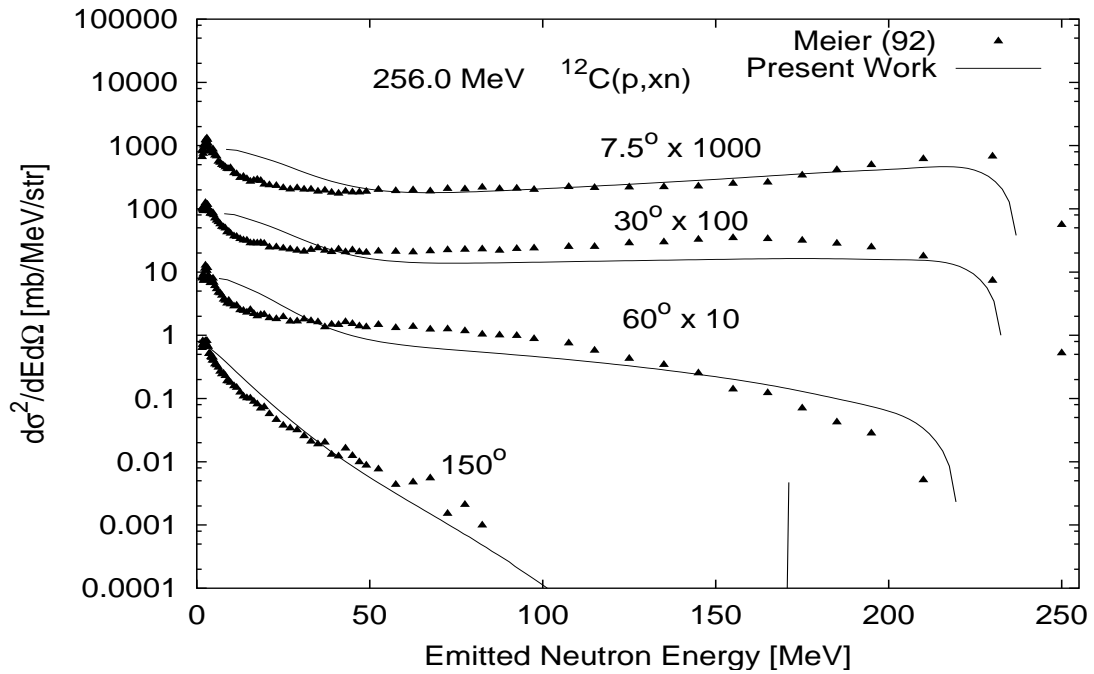


Figure 3: Evaluated $^{12}\text{C}(p, xn)$ double-differential neutron emission spectra compared with experimental data [7] at 256 incident energy

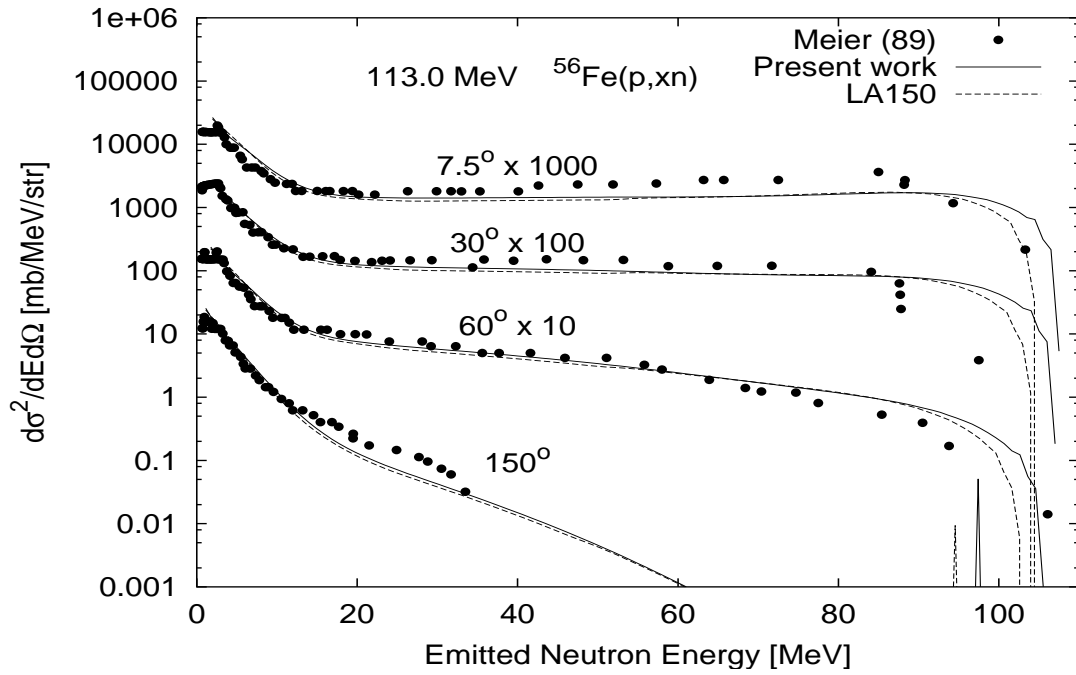


Figure 4: Evaluated $^{56}\text{Fe}(p, xn)$ double-differential neutron emission spectra compared with experimental data [6] and LA150 at 113 incident energy

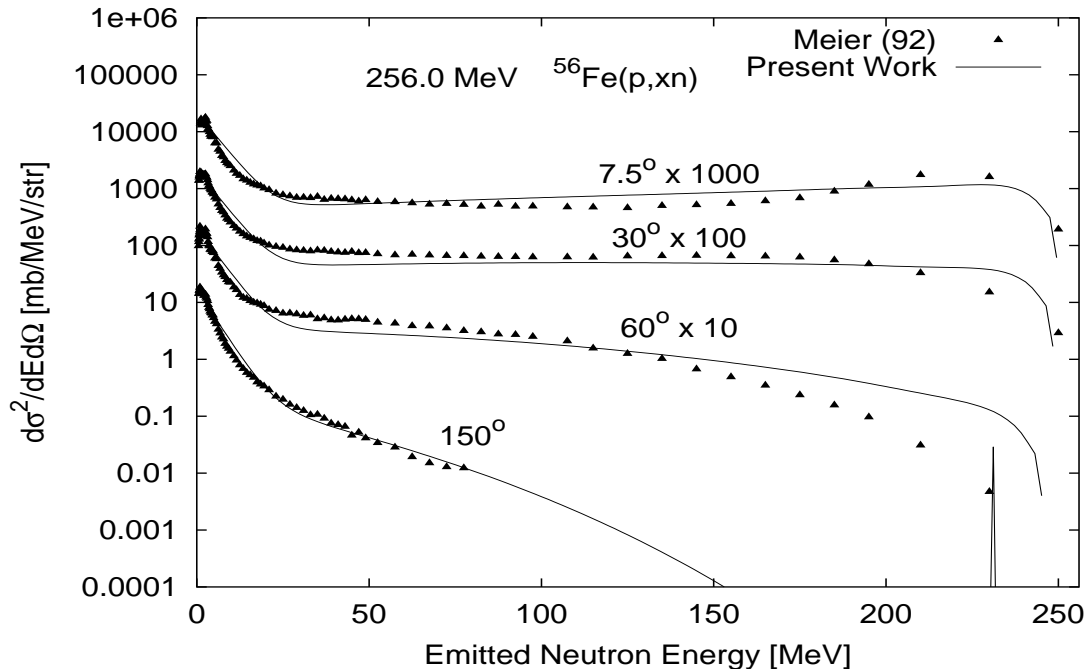


Figure 5: Evaluated $^{56}\text{Fe}(p, xn)$ double-differential neutron emission spectra compared with experimental data [7] at 256 incident energy

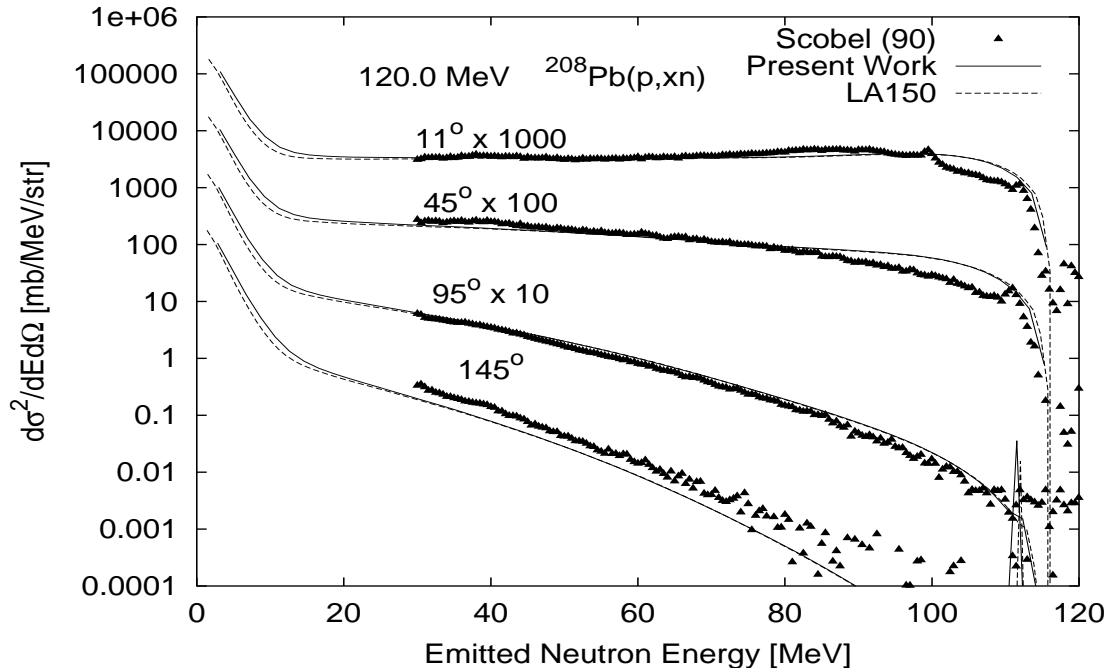


Figure 6: Evaluated $^{208}\text{Pb}(p, xn)$ double-differential neutron emission spectra compared with experimental data [6] and LA150 at 120 MeV incident energy

shows a comparison among our evaluation, LA150, and the measurements of Scobel et al. [6] for double-differential neutron emission spectra at 11, 45, 95 and 145 degrees for 120 MeV of incident proton. Agreement is fairly good over the whole emission energies and angles except at 145 degree, where the calculated double differential emission cross sections are lower than the measured data.

For incident proton energy above 150 MeV, Our evaluations are compared in Fig. 7 with the measurements of Scobel et al. [8] for 160.3 MeV, and in Fig. 8 with the measurements of Stamer et al. [9] for 256 MeV. Again, the evaluated double differential neutron emission spectra reproduce the measured data quite well, except for the high energy emission tail at 60 and 150 degree angles for 256 MeV of incident proton.

3.4 SUMMARY

Below 150 MeV of incident protons, no significant differences are noticed among our evaluation, the LA150, and the measurements, since the reference measurements and theoretical models are same for our evaluation and the LA150 except the neutron and proton optical model parameters, whose effects are assumed to be washed out in the inclusive emission spectra.

Meanwhile, our evaluations for energies up to 250 MeV are made on the same reaction models as adopted in the LA150 evaluation, but with the utilization of the optical model parameters of neutron and proton validated for incident energies up to 400 MeV, and benchmark with appropriate reference measurements for energies above 150 MeV. As

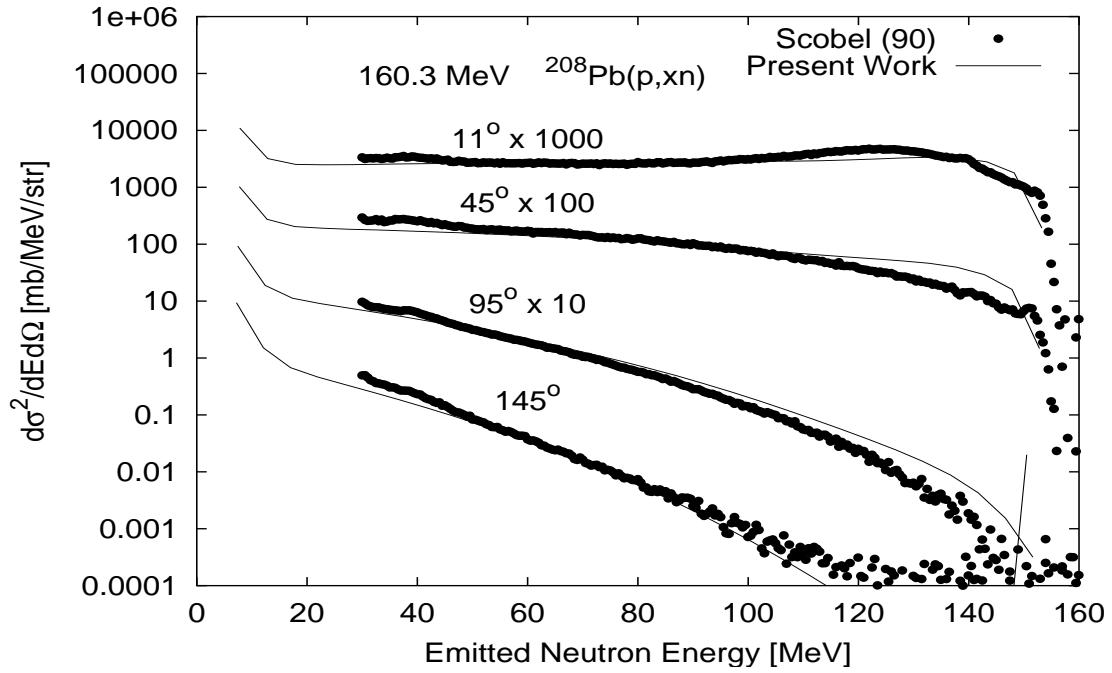


Figure 7: Evaluated $^{208}\text{Pb}(p, xn)$ double-differential neutron emission spectra compared with experimental data [8] at 160.3 MeV incident energy

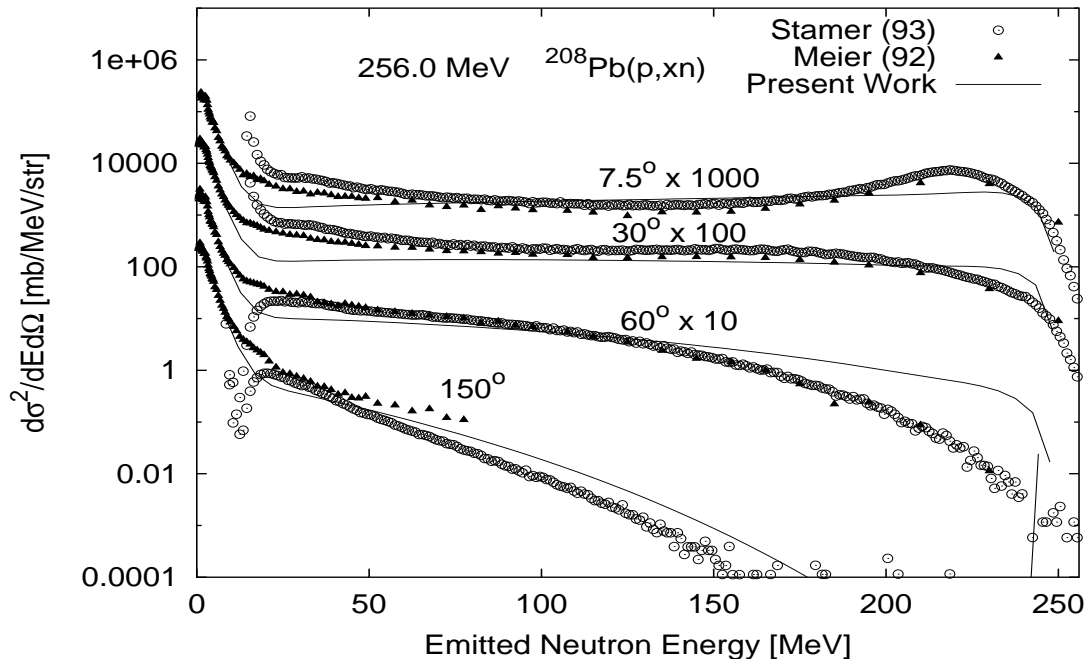


Figure 8: Evaluated $^{208}\text{Pb}(p, xn)$ double-differential neutron emission spectra compared with experimental data [7, 9] at 256 MeV incident energy

results, fairly good agreement has been achieved in the neutron double differential emission spectra for entire emission energy and angle range, except at some backward angles.

ACKNOWLEDGEMENTS

This work was supported by the Korea Ministry of Science and Technology as one of the long-term nuclear R&D programs.

References

1. Y. O. Lee and et al., "High Energy Nuclear Data Evaluations for Neutron-, Proton-, and Photon-Induced Reactions at KAERI," in *Proc. of the International Conference on Nuclear Data for Science and Technology*, Oct., Tsukuba, Japan (2001).
2. Y. Cho, Y. Lee, and J. Chang, "KASKAD: Deterministic Two-Dimensional Neutral and Charged Particle Transport Code System," in *Proc. of the Korean Nuclear Society Fall Meeting*, Suwon, Korea, April (2001).
3. M. Chadwick and et al., "Cross Section Evaluations to 150 MeV for Accelerator-Driven Systems and Implementation in MCNPX," *Nucl. Sci. Eng.*, **vol. 131**, p. 293 (1999).
4. Y. O. Lee, J. Chang, and M. Kim, "Parameterization and Optical Model Analyses of Proton-Nucleus Cross Sections for Space Shielding," *IEEE Transactions on Nuclear Science*, **vol. 47**, no. 6, p. 2435 (2000).
5. Y. O. Lee, T. Fukahori, J. Chang, and S. Chiba, "Optical model potential search for neutron- and proton induced reactions of ^{12}C , ^{16}O , ^{27}Al , ^{56}Fe , ^{90}Zr and ^{208}Pb up to 250 MeV," in *Proc. of PHYSOR 2000: ANS International Topical Meeting on Advances in Reactor Physics and Mathematics and Computation into the Next Millennium*, Pittsburgh, Pennsylvania, U.S.A, May 7-12, 2000 (2000).
6. M. Meier, D. Clark, C. Goulding, J. Mcclelland, G. Morgan, C. Moss, and W. Amin, "Differential neutron production cross sections and neutron yield from stopping-length targets for 113 MeV," *Nucl. Sci. Eng.*, **vol. 102**, p. 310 (1989). EXFOR O0100.
7. M. Meier, W. Amian, C. Goulding, G. Morgan, and C. Moss, "Differential neutron production cross sections for 256-MeV protons," *Nucl. Sci. Eng.*, **vol. 110**, p. 289 (1992). EXFOR C0168.
8. W. Scobel, M. Trabandt, M. Blann, B. Pohl, B. Remington, R. Byrd, C. Foster, R. Bonetti, C. Chiesa, and S. Grimes, "Preequilibrium (p,n)reaction As a probe for the effective nucleon-nucleon interaction in multistep direct processes," *Phys. Rev. C*, **vol. 41**, p. 2010 (1990). EXFOR O0181.
9. S. Stamer, W. Scobel, W. Amian, R. Byrd, R. Haight, J. Ullmann, R. Bauer, M. Blann, B. Pohl, J. Bisplinghoff, and R. Bonetti, "Double differential cross sections for neutron

- emission induced by 256 MeV and 800 MeV protons,” *Phys. Rev. C*, **vol. 47**, p. 1647 (1993). EXFOR O0182.
10. S. Stamer, W. Scobel, W. Amian, R. Byrd, M. Blann, B. Pohl, J. Bisplinghoff, and R. Bonetti, “Double differential cross sections for neutron emission induced by 256 MeV and 800 MeV protons,” *Phys. Rev. C*, **vol. 47**, p. 1647 (1993). EXFOR C0511.
 11. OECD/NEA (WWW address: <http://www.nea.fr>).
 12. P. G. Young, E. D. Arthur, and M. B. Chadwick, “Comprehensive nuclear model calculations: Theory and use of the GNASH code,” in *Proc. of the IAEA Workshop on Nuclear Reaction Data and Nuclear Reactors - Physics, Design, and Safety* (A. Gandini and G. Reffo, eds.), (Singapore), pp. 227–404, Trieste, Italy, April 15 - May 17, 1996, World Scientific Publishing, Ltd. (in press).
 13. R. B. Firestone and V. S. Shirley, *Table of Isotopes, 8th edition*. New York, NY: John Wiley and Sons (1996).
 14. G. Audi and A. Wapstra *Nucl. Phys.*, **vol. A595**, p. 409 (1995).
 15. P. Moeller, J. Nix, W. Myers, and W. Swiatecki *Atomic Data and Nuclear Data Tables*, **vol. 59**, p. 185 (1995).
 16. A. V. Ignatyuk, G. N. Smirenkin, and A. Tishin, “Phenomenological Description of the Energy Dependence of the Level Density Parameter,” *Sov. J. Nucl. Phys.*, **vol. 21**, pp. 255–257 (1975).